

Design of Safety, High Step-Up DC–DC Converter for AC PV Module Application

B. Ashok¹ J. Mohan²

¹PG Student (Power Electronics & Drives), Dept of EEE, Ranganathan Engineering College, Coimbatore,

²Assistant Professor, Dept of EEE, Ranganathan Engineering College, Coimbatore, Tamilnadu. India.

Abstract: In current scenario, the world is giving importance to renewable energy power generation is to meet electricity demand. The power generated by using Photovoltaic (PV) panel has been connected to the applications, through the DC-DC converter and DC-AC inverter. This paper proposes a new high step up DC-DC converter with floating active switch isolates the energy from the PV panel when the AC module is off & also act as high state drive. It also regulates the DC interface between the DC-AC converters. The high step up voltage conversion ratio is obtained with numerous turns ratio of a coupled inductor and also with appropriate duty ratios. The energy stored in the leakage inductor, will be recycled by magnetizing inductor L_M present in the coupled inductor to the R load through the output capacitor C_3 . By applying 15V input voltage and 200V output voltage is obtained, designed converter circuit attains 98W as output power. This is better than conventional convert model efficiency.

Key words: Active floating switch, AC module, Coupled inductor, high step up Voltage conversion ratio .

1. Introduction

The uses of non conventional energy sources like solar energy requires a large step up conversion of their low voltage level to the required amount of voltage. A higher DC-link voltage is obtained by serial connection of large number of PV arrays.

Through the DC-AC inverter the DC voltage can be utilized for the main electricity [4], [5]. An AC module is a micro inverter configured on the rear bezel of PV panel, this will immunizes against the yield loss by shadow effect. The prior works have proposed the converter shown in fig 1 with single switch and fewer components to fit the dimensions of the bezel of the ac module, but their efficiency levels are low. The maximum power point voltage (MPPT) range is 12V to 40V which will give as input for the output power capacity range of 50W to 250W.

In case if low voltage derived from the PV panel, then it is difficult for the AC module to reach the high efficiency [8]. Employing a high step-up DC-DC converter in front of the inverter, this provides the stable DC link to the inverter & power conversion efficiency from one level to another level.

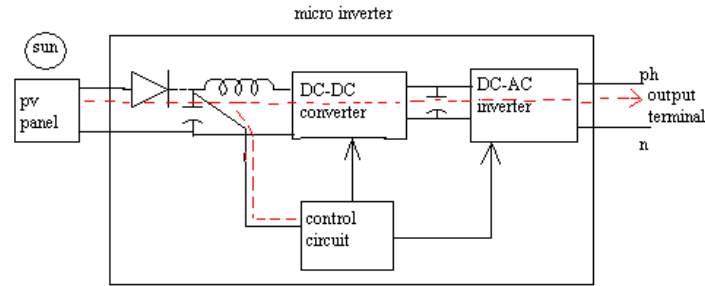


Fig 1 conventional method without floating switch

During day light, installation of PV panel generation system [1], [2], the potential difference could pose hazards to both the worker and the facilities while installing the AC module. When the AC module is off, a floating active switch is designed to isolate the DC from the PV panel, for grid as well as non operating condition. This isolation ensures the operation of the internal components without any residential energy being transferred to the terminals, which could be unsafe. Use of active clamp technique [25] not only recycles the leakage inductor energy but also it constraints the voltage stress across the switch. This means the coupled inductor employed in voltage liter or voltage multiplier technique in a circuit [11].

The DC-DC converter requires a large step-up voltage conversion from low voltage obtained from the panel low voltage to the required voltage level for the application. In the previous research on various converters employed with the switched – capacitor type,[3] the voltage-lift type,[4] the capacitor-diode voltage multiplier [5],[6] and the boost type integrated with coupled inductor [23] these converters by increasing turns ratio of coupled inductor obtain higher voltage gain than conventional boost converter for high step-up applications. Some converters successfully combined boost and flyback converters [21],[22], some converters, since various converter combinations are developed to carryout high step up voltage gain by using the coupled-inductor technique [12],[19]. The efficiency and voltage gain of the DC-DC boost converter are constrained by either switches or the reverse recovery issues of the diodes [21], [22].

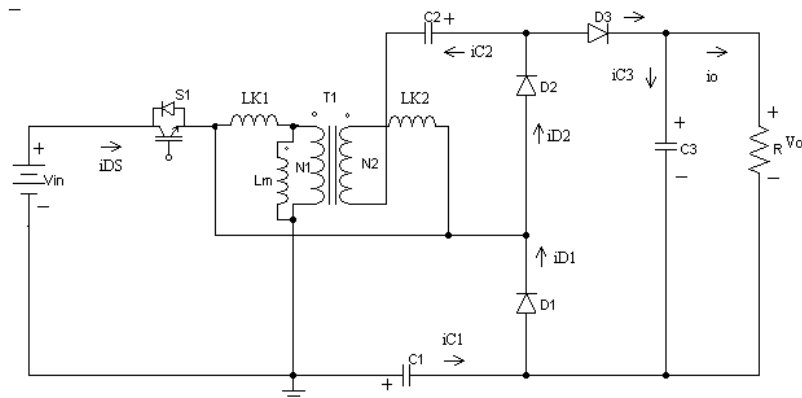


Fig 2 circuit diagram of proposed converter

The circuit diagram of proposed converter is shown in figure.2. The primary winding $N1$ of a coupled inductor $T1$ and capacitor $C1$ and diode $D1$ receive leakage inductor energy from $N1$. The secondary winding $N2$ of Coupled inductor $T1$ is connected with another pair of capacitor $C2$ and diode $D2$, which are in series

with N1 in order to further enlarge the boost voltage. The floating active switch S1 is connected to T1. The diode D3 is a diode rectifier which is connected to the output capacitor C3 and R load.

2. Operation of the Proposed Converter

The following assumptions are made to analysis the circuit diagram of the proposed converter.

- 1) Expect the leakage inductance of coupled inductor T1, all the components are ideal.
- 2) The snubber capacitance of S1, The on-state resistance $R_{DS(on)}$ are neglected.
- 3) The capacitors C1, C2, C3 are sufficiently large that the voltages across them are considered to be constant.
- 4) The coupled inductor T1 & ESR of capacitors C1 C2 C3 and the parasitic resistance are neglected.
- 5) The turn ratio n of the coupled inductor T1 windings is equal to $N2 / N1$.

The proposed converter will be worked in two modes of operation, they are

- (i) Continuous conduction mode (CCM)
- (ii) Discontinuous conduction mode (DCM).

2.1 Continuous Conduction Mode Operation (CCM) of proposed converter

Mode I [$t_0 \leq t \leq t_1$]: In this interval, when S1 is turned ON, the magnetizing inductor L_m continuously charges capacitor C2 through T1. Switch S1 and diode D2 are conducting. The source voltage V_{in} crosses magnetizing inductor L_m and primary leakage inductor L_{k1} due to the current i_{Lm} is decreasing; magnetizing inductor L_m is still transferring its energy through coupled inductor T1 to charge switched capacitor C2, but the energy is decreasing. The charging current i_{D2} and i_{C2} are decreasing. The secondary leakage inductor current i_{Lk2} is declining as equal to i_{Lm} / n . Once the increasing i_{Lk1} equals decreasing i_{Lm} at $t = t_1$, this mode ends.

Mode II [$t_1 \leq t \leq t_2$]: In this interval, N2 is series connected with source energy V_{in} . C1, and C2 to charge output capacitor C3 and load R, and also magnetizing inductor L_m is also receiving energy from V_{in} . Where switch S1 remains ON, only diode D3 is conducting. The i_{Lm} , i_{Lk1} , and i_{D3} are increasing because the V_{in} is crossing L_{k1} , L_m , and primary winding N1. L_m and L_{k1} are storing energy from V_{in} , and also V_{in} is also serially connected with secondary winding N2 of coupled inductor T1, capacitors C1, and C2, and then discharges their energy to capacitor C3 and load R. The i_{in} , i_{D3} and discharging current i_{C1} and i_{C2} are increasing. This mode ends when switch S1 is turned OFF at $t = t_2$.

Mode III [$t_2 \leq t \leq t_3$]: In this interval, when switch S1 is OFF, secondary leakage inductor L_{k2} will charge C3. Only diode D1 and D3 are conducting. The energy stored in leakage inductor L_{k1} flows through diode D1 to charge capacitor C1 instantly when S1 is OFF and also the energy of secondary leakage inductor L_{k2} is series connected with C2 to charge output capacitor C3 and the load. Because leakage inductance L_{k1} and L_{k2} are smaller than L_m , i_{Lk2} rapidly decreases, but i_{Lm} is increasing due to magnetizing inductor L_m is receiving energy from L_{k1} . Current i_{Lk2} decreases until it reaches zero, this mode ends at $t = t_3$.

Mode IV [$t_3 \leq t \leq t_4$]: In this interval, the energy stored in magnetizing inductor L_m is released to C_1 and C_2 simultaneously. Only diodes D_1 and D_2 are conducting. Currents i_{Lk1} and i_{D1} are continually decreased due to the leakage energy still flowing through diode D_1 is charging capacitor C_1 . The L_m is delivers energy through T_1 and D_2 to charge capacitor C_2 . The energy stored in capacitor C_3 is constantly discharges to the load R . These energy transfers result in decreases in i_{Lk1} and i_{Lm} but increases in i_{Lk2} . This mode ends when current i_{Lk1} is zero, at $t = t_4$.

Mode V [$t_4 \leq t \leq t_5$]: In this interval, only magnetizing inductor L_m is constantly discharges its energy to C_2 in which only diode D_2 is conducting. The i_{Lm} is decreasing due to the magnetizing inductor energy flowing through the coupled inductor T_1 to secondary winding N_2 , so D_2 continues to charge capacitor C_2 . The energy stored in capacitor C_3 is constantly discharges to the load R . This mode ends when switch S_1 is turned ON at the beginning of the next switching period.

2.2. Dis-Continuous Conduction Mode Operation of proposed converter

Mode I [$t_0 \leq t \leq t_1$]: In this interval, N_2 , C_1 , and C_2 to charge output capacitor C_3 and load R are series connected with source energy V_{IN} , and also magnetizing inductor L_m is also receiving energy from V_{in} . which depicts that switch S_1 remains ON, and only diode D_3 is conducting. The i_{Lm} , i_{Lk1} , and i_{D3} are increasing because the V_{in} is crossing $Lk1$, L_m , and primary winding N_1 . L_m and $Lk1$ are storing energy from V_{in} , meanwhile, V_{in} also is serially connected with secondary winding N_2 of coupled inductor T_1 , capacitors C_1 , and C_2 , then they all discharge their energy to capacitor C_3 and load R . The i_{in} , i_{D3} and discharging current i_{C1} and i_{C2} are increasing. This mode ends when Switch S_1 is turned OFF at $t = t_1$.

Mode II [$t_1 \leq t \leq t_2$]: In this interval, when switch S_1 is OFF, secondary leakage inductor $Lk2$ keeps charging C_3 . And only diode D_2 and D_3 are conducting. When S_1 is OFF, The energy stored in leakage inductor $Lk1$ flows through diode D_1 to charge capacitor C_1 . in the meantime, the energy of secondary leakage inductor $Lk2$ is series-connected with C_2 to charge output capacitor C_3 and the load. as leakage inductance $Lk1$ and $Lk2$ are lesser than L_m , i_{Lk2} decreases rapidly, but i_{Lm} is increasing because magnetizing inductor L_m is receiving energy from $Lk1$. Current i_{Lk2} reduces down to zero, and this mode ends at $t = t_2$.

Mode III [$t_2 \leq t \leq t_3$]: In this interval, only diodes D_1 and D_2 are conducting, the energy stored in coupled inductor T_1 is release to C_1 and C_2 . Currents i_{Lk1} and i_{D1} are constantly decreased as leakage energy still flowing through diode D_1 keeps charging capacitor C_1 . The L_m is deliver its energy through T_1 and D_2 to charge capacitor C_2 . The energy stored in capacitor C_3 is constantly discharged to the load R . These energy transfers cause decreases in i_{Lk1} and i_{Lm} but increases in i_{Lk2} . This mode ends when current i_{Lk1} reaches zero at $t = t_3$.

Mode IV [$t_3 \leq t \leq t_4$]: In this interval, only magnetizing inductor L_m is continually release its energy to C_2 , also only diode D_2 is conducting. The i_{Lm} is decreasing due to the magnetizing inductor energy flowing through the coupled inductor T_1 to secondary winding N_2 , and D_2 continues to charge capacitor C_2 . The energy

stored in capacitor C3 is constantly discharged to the load R. This mode ends when current i_{Lm} reach zero at $t = t_4$.

Mode V [$t_4 \leq t \leq t_5$]: In this interval, all components are turned OFF, only the energy stored in capacitor C3 is constant to be discharged to the load R. When switch S1 is turned ON this modes ends and the beginning of the next switching period.

3. Steady state analysis of Proposed Converter

3.1. CCM Operation

To simplify the analysis, the leakage inductances on the secondary and primary sides are neglected.

When S1 is turned ON the voltage across magnetizing inductance LM & N2

$$V_{Lm} = V_{in} \quad (1)$$

$$V_{N2} = nV_{in}. \quad (2)$$

During S2 OFF the voltage across magnetizing inductance LM & N2

$$V_{Lm} = -V_{C1} \quad (3)$$

$$V_{N2} = -V_{C2}. \quad (4)$$

The voltages across capacitors C1 and C2 are obtained as

$$V_{C1} = D / (1 - D) V_{in} \quad (5)$$

$$V_{C2} = nd / (1 - D) V_{in}. \quad (6)$$

$$V_O = V_{in} + V_{N2} + V_{C2} + V_{C1} \quad (7)$$

The DC voltage gain (MCCM) is:

$$MCCM = (V_O / V_{in}) = ((1 + n) / (1 - D)) \quad (8)$$

3.2. DCM Operation

To simplify the analysis, the leakage inductances on the secondary and primary sides are neglected.

When S1 is turned ON the voltage across magnetizing inductance LM & N2

$$V_{Lm} = V_{in} \quad (9)$$

$$V_{N2} = nV_{in}. \quad (10)$$

During S2 OFF the voltage across magnetizing inductance LM & N2

$$V_{Lm} = -V_{C1} \quad (11)$$

$$-V_{N2} = V_{C2}. \quad (12)$$

The voltages across capacitors C3 and C4 are obtained as

$$V_{C1} = (D / DL) V_{in} \quad (13)$$

$$V_{C2} = nD / (DL) V_{in} \quad (14)$$

$$V_O = (n + 1) / (D + DL) DL V_{in}. \quad (16)$$

$$MDCM = (V_O / V_{in}) = (n + 1) + \sqrt{(n + 1)^2 + (2D^2 / \tau L) / 2} \quad (17)$$

3.3 Boundary condition mode (BCM)

Normalized magnetizing inductor time constant τ_{LB} to be depicted as

$$\tau_{LB} = (D(1 - D)^2) / 2(1 + n)^2 = D / 2(MCCM)^2$$

Once the τ_{Lm} is higher than boundary curve τ_{LmB} , the proposed converter operates in CCM.

3. Simulation Result

The simulation is done using MATLAB software, the results obtained from the proposed converter with the electrical specifications of the circuit components with an applied input DC voltage of $V_{in}=15V$, and output DC voltage V_{out} in CCM $V_{out}=201V$ and DCM $V_{out}=287V$. The output current $I_{out}=0.5A$. Switching frequency $f=50\text{ kHz}$, load resistance of $R=400\ \Omega$. The capacitor value of $C_1=C_2=47\mu F$ and $C_3=220\mu F$, the switch S_1 used for the simulation is IGBT, for recycle and rectify diodes are used. The turns ratio n of the mutual inductor is $n=5$, and the duty ratio D is derived as 50%. The magnetizing inductor $L_m > 30.54$ of coupled inductor for the full load. The proposed converter obtains the wide range of efficiency when fading of sunlight occurs. The maximum full load efficiency of the proposed converter at continuous conduction mode is given by 98%, which is higher than conventional schemes.

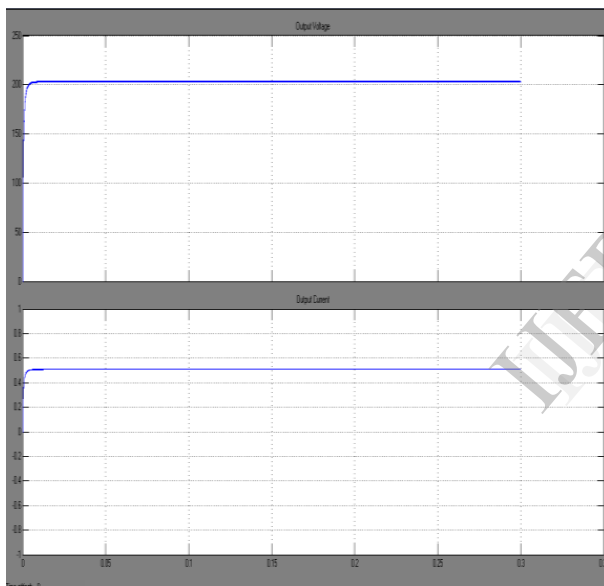


Fig 3 Output waveform for CCM mode

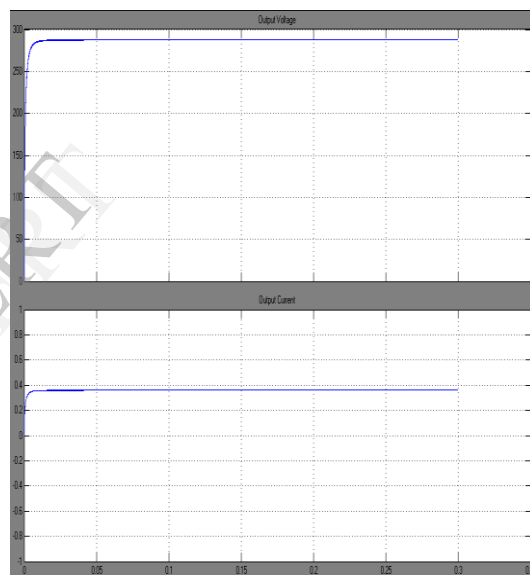


fig 4 output waveform in DCM mode

The fig 3 shows output current & output voltage waveform the output voltage $V_{out}=201V$ & $I_{out}=0.5A$ in continuous conduction mode. Fig 4 shows output voltage & current $V_{out}=287V, I_{out}=0.5A$ in discontinuous mode.

The fig 5 shows, the voltage & current waveform of the switch S_1 , current in capacitor C_1, C_2 the current in diode D_1, D_2, D_3 in DCM mode of operation and also the fig 6 shows the voltage & current waveform of switch S_1 , current capacitor C_1, C_2 the current in D_1, D_2, D_3 in CCM mode of operation.

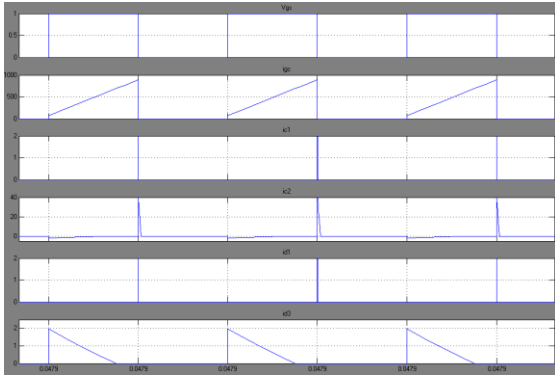


Fig 5 output wave form in DCM mode

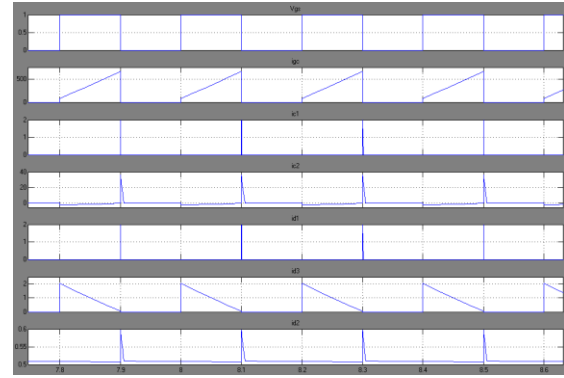


Fig 6 output wave form in CCM mode

4. CONCLUSION

The voltage stress across the switch is controlled by leakage inductor which effectively recycles energy in coupled inductor. During OFF state of AC module the floating switch will protect from residential energy & gives safety for the users as well as components from electrical hazards. High step up voltage gain is obtained, without numerous turns ratio and extreme duty ratio in coupled inductor $n=5$ and duty ratio $D=55\%$ in the converter. During fading sunlight PV module harvest more energy due to small efficiency variation.

References

- [1] J. J. Bzura, "The ac module: An overview and update on self-contained modular PV systems," in *Proc. IEEE Power Eng. Soc. Gen. Meeting*, Jul. 2010, pp. 1–3.
- [2] B. Jablonska, A. L. Kooijman-van Dijk, H. F. Kaan, M. van Leeuwen, G. T. M. de Boer, and H. H. C. de Moor, "PV-PRIVATE project at ECN, five years of experience with small-scale ac module PV systems," in *Proc. 20th Eur. Photovoltaic Solar Energy Conf.*, Barcelona, Spain, Jun. 2005, pp. 2728–2731.
- [3] T. Umeno, K. Takahashi, F. Ueno, T. Inoue, and I. Oota, "A new approach to low-ripple-noise switching converters on the basis of switched-capacitor converters," in *Proc. IEEE Int. Symp. Circuits Syst.*, Jun. 1991, pp. 1077–1080.
- [4] B. Axelrod, Y. Berkovich, and A. Ioinovici, "Transformerless dc–dc converters with a very high dc line-to-load voltage ratio," in *Proc. IEEE Int. Symp. Circuits Syst. (ISCAS)*, 2003, vol. 3, pp. 435–438.
- [5] H. Chung and Y. K. Mok, "Development of a switched-capacitor dc–dc boost converter with continuous input current waveform," *IEEE Trans. Circuits Syst. I, Fundam. Theory Appl.*, vol. 46, no. 6, pp. 756–759, Jun. 1999.
- [6] T. J. Liang and K. C. Tseng, "Analysis of integrated boost-flyback step-up converter," *IEE Proc. Electrical Power Appl.*, vol. 152, no. 2, pp. 217–225, Mar. 2005.
- [7] T. Shimizu, K. Wada, and N. Nakamura, "Flyback-type single-phase utility interactive inverter with power pulsation decoupling on the dc input for an ac photovoltaic module system," *IEEE Trans. Power Electron.*, vol. 21, no. 5, pp. 1264–1272, Jan. 2006.
- [8] C. Rodriguez and G. A. J. Amaratunga, "Long-lifetime power inverter for photovoltaic ac modules," *IEEE Trans. Ind. Electron.*, vol. 55, no. 7, pp. 2593–2601, Jul. 2008.
- [9] S. B. Kjaer, J. K. Pedersen, and F. Blaabjerg, "A review of single-phase grid-connected inverters for photovoltaic modules," *IEEE Trans. Ind. Appl.*, vol. 41, no. 5, pp. 1292–1306, Sep./Oct. 2005.
- [10] M. Zhu and F. L. Luo, "Voltage-lift-type cuk converters: Topology and analysis," *IET Power Electron.*, vol. 2, no. 2, pp. 178–191, Mar. 2009.

- [11] J. W. Baek, M. H. Ryoo, T. J. Kim, D. W. Yoo, and J. S. Kim, "High boost converter using voltage multiplier," in *Proc. IEEE Ind. Electron. Soc. Conf. (IECON)*, 2005, pp. 567–572.
- [12] J. Xu, "Modeling and analysis of switching dc–dc converter with coupled inductor," in *Proc. IEEE 1991 Int. Conf. Circuits Syst. (CICCAS)*, 1991, pp. 717–720.
- [13] S. H. Park, S. R. Park, J. S. Yu, Y. C. Jung, and C. Y. Won, "Analysis and design of a soft-switching boost converter with an HI-Bridge auxiliary resonant circuit," *IEEE Trans. Power Electron.*, vol. 25, no. 8, pp. 2142–2149, Aug. 2010.
- [14] G. Yao, A. Chen, and X. He, "Soft switching circuit for interleaved boost converters," *IEEE Trans. Power Electron.*, vol. 22, no. 1, pp. 80–86, Jan. 2007.
- [15] Y. Park, S. Choi, W. Choi, and K. B. Lee, "Soft-switched interleaved boost converters for high step-up and high power applications," *IEEE Trans. Power Electron.*, vol. 26, no. 10, pp. 2906–2914, Oct. 2011.
- [16] Y. Zhao, W. Li, Y. Deng, and X. He, "Analysis, design, and experimentation of an isolated ZVT boost converter with coupled inductors," *IEEE Trans. Power Electron.*, vol. 26, no. 2, pp. 541–550, Feb. 2011.
- [17] T. J. Liang, S. M. Chen, L. S. Yang, J. F. Chen, and A. Ioinovici, "Ultra large gain step-up switched-capacitor dc–dc converter with coupled inductor for alternative sources of energy," *IEEE Trans. Circuits Syst. I*, to be published.
- [18] L. S. Yang and T. J. Liang, "Analysis and implementation of a novel bidirectional dc–dc converter," *IEEE Trans. Ind. Electron.*, vol. 59, no. 1, pp. 422–434, Jan. 2012.
- [19] W. Li and X. He, "Review of non-isolated high-step-up dc/dc converters in photovoltaic grid-connected applications," *IEEE Trans. Ind. Electron.*, vol. 58, no. 4, pp. 1239–1250, Apr. 2011.
- [20] C. Restrepo, J. Calvente, A. Cid, A. El Aroudi, and R. Giral, "A noninverting buck-boost dc–dc switching converter with high efficiency and wide bandwidth," *IEEE Trans. Power Electron.*, vol. 26, no. 9, pp. 2490–2503, Sep. 2011.
- [21] K. B. Park, G. W. Moon, and M. J. Youn, "Nonisolated high step-up boost converter integrated with SEPIC converter," *IEEE Trans. Power Electron.*, vol. 25, no. 9, pp. 2266–2275, Sep. 2010.
- [22] L. S. Yang, T. J. Liang, and J. F. Chen, "Transformerless dc–dc converters with high step-up voltage gain," *IEEE Trans. Ind. Electron.*, vol. 56, no. 8, pp. 3144–3152, Aug. 2009.
- [23] N. Pogaku, M. Prodanovic, and T. C. Green, "Modeling, analysis and testing of autonomous operation of an inverter-based microgrid," *IEEE Trans. Power Electron.*, vol. 22, no. 2, pp. 613–625, Mar. 2007.
- [24] H. Mao, O. Abdel Rahman, and I. Batarseh, "Zero-voltage-switching dc–dc converters with synchronous rectifiers," *IEEE Trans. Power Electron.*, vol. 23, no. 1, pp. 369–378, Jan. 2008.
- [25] J. M. Kwon and B. H. Kwon, "High step-up active-clamp converter with input-current doubler and output-voltage doubler for fuel cell power systems," *IEEE Trans. Power Electron.*, vol. 24, no. 1, pp. 108–115, Jan. 2009.
- [26] S. Dwari and L. Parsa, "An efficient high-step-up interleaved dc–dc converter with a common active clamp," *IEEE Trans. Power Electron.*, vol. 26, no. 1, pp. 66–78, Jan. 2011.

B.ASHOK presently pursuing his M.E in power electronics & drives, in Ranganathan Engineering College, Coimbatore. His area of interest is power electronic inverters & converters.

J.MOHAN presently working as assistant professor in Ranganathan Engineering College, Coimbatore. His area of interest is power electronic converter & inverters, AC & DC drives, power quality.